Journal of Hazardous Materials 192 (2011) 1088–1093

Contents lists available at ScienceDirect

Journal of Hazardous Materials

journal homepage: www.elsevier.com/locate/jhazmat

Strong adsorption of chlorotetracycline on magnetite nanoparticles

Di Zhang[a,b], Hongyun Niu[a], Xiaole Zhang[a,c], Zhaofu Meng[b], Yaqi Cai[a,*]

[a] State Key Laboratory of Environmental Chemistry and Ecotoxicology of Research Center for Eco-Environmental Sciences, Chinese Academy of Sciences, Beijing 100085, China
[b] College of Science, Northwest A&F University, Yangling, Shaanxi 712100, China
[c] College of Chemical Engineering and Biological Technology, Hebei United University, Tangshan, Hebei 063000, China

ARTICLE INFO

Article history:
Received 8 January 2011
Received in revised form 6 June 2011
Accepted 7 June 2011
Available online 12 June 2011

Keywords:
Fe_3O_4 nanoparticles
Chlorotetracycline
Adsorption
Regeneration

ABSTRACT

In this work, environmentally friendly magnetite nanoparticles (Fe_3O_4 MNPs) were used to adsorb chlorotetracycline (CTC) from aqueous media. Fe_3O_4 MNPs exhibit ultrahigh adsorption ability to this widely used antibiotic. The adsorption behavior of CTC on Fe_3O_4 MNPs fitted the pseudo-second-order kinetics model, and the adsorption equilibrium was achieved within 10 h. The maximum Langmuir adsorption capacity of CTC on Fe_3O_4 (476 mg g^{-1}) was obtained at pH 6.5. Thermodynamic parameters calculated from the adsorption data at different temperature showed that the adsorption reaction was endothermic and spontaneous. Low concentration of NaCl and foreign divalent cations hardly affected the adsorption. Negative effect of coexisting humic acid (HA) on CTC adsorption was also observed when the concentration of HA was lower than 20 mg L^{-1}. But high concentration of HA (>20 mg L^{-1}) increased the CTC adsorption on Fe_3O_4 MNPs. The matrix effect of several environmental water samples on CTC adsorption was not evident. Fe_3O_4 MNPs were regenerated by treatment with H_2O_2 or calcination at 400 °C in N_2 atmosphere after separation from water solution by an external magnet. This research provided a high efficient and reusable adsorbent to remove CTC selectively from aqueous media.

1. Introduction

Antibiotics have been widely used in human and veterinary medicine for about 70 years [1]. In China, the annual usage of tetracyclines (TCs), a kind of important antibiotic, was about 9413 tons in 1999 and the production of oxytetracycline was about 10000 tons in 2003 [2]. Most of the TCs were excreted to environment without metabolism and assimilation [3]. Residues of tetracyclines have been frequently detected in various environmental water samples [4,5]. The presence of TCs in environment has raised significant concern because high concentration of TCs is potentially hazardous to sludge bacteria and non-target organisms in aqueous environment [6–8]. Most importantly, the emergence of superbugs with it has threatened the public health significantly and caused a psychic scare [9]. Therefore, elimination of TCs from environment is extremely urgent to reduce the potential health risk and ecological risk of TCs.

TC's electron-rich ketone, amide, and hydroxyl groups contribute to forming stable metal–ligand complexes with multivalent cations [10,11]. Recently, the elimination of TCs by minerals and metal oxides has been investigated [12,13]. Hydrous oxides of iron are important components of environmental minerals which are considered as major adsorbents for many inorganic and organic contaminants [14]. Tanis et al. [15] investigated the adsorption behavior of TCs on naturally occurring iron-bearing minerals such as iron oxides-coated quartz. These studies reveal the excellent adsorption ability of TCs on iron oxides. However, the study about the adsorption of TCs on nano-scaled iron oxide is rare.

Fe_3O_4 MNPs have attracted attention in the field of pollutant adsorption and environmental remediation owing to the large surface area, high adsorption ability, sufficient stability, easy preparation, convenient operation and facile recycling. The potential applications of Fe_3O_4 MNPs for the removal of arsenic, Ni(II), Cu(II), Cd(II), Cr(VI), palladium(II), rhodium(III), platinum(IV), and neutral red dye from aqueous solution have been investigated [16–18]. As a result, Fe_3O_4 MNPs show large adsorption capacity and fast adsorptive rate to these contaminants. In this study, Fe_3O_4 MNPs were synthesized and used to adsorb chlorotetracycline (CTC) from environmental water samples. The adsorption kinetics and effects of solution pH, temperature, ions strength, coexisting cations, HA on the adsorption of CTC were investigated by batch experiments with spiked deionized water. Regeneration of Fe_3O_4 MNPs was also carried out to examine its reusability.

2. Experimental

All chemicals were of analytical reagent grade and used without further purification. The information of chemicals and details of

* Corresponding author at: Research Center for Eco-Environmental Sciences, Chinese Academy of Sciences, P.O. Box 2871, Beijing 100085, China.
Tel.: +86 010 62849182; fax: +86 010 62849239.
E-mail address: caiyaqi@rcees.ac.cn (Y. Cai).

0304-3894/$ – see front matter © 2011 Elsevier B.V. All rights reserved.
doi:10.1016/j.jhazmat.2011.06.015

Table 1
Properties of synthesized Fe_3O_4 MNPs.

Adsorbent	Mean diameter (nm)	Surface area ($m^2\,g^{-1}$)	pH_{pzc}	Saturation magnetic intensity ($emu\,g^{-1}$)	Element content (at%)		Site density ($Fe\,(nm^2)^{-1}$)
					O	Fe	
Fe_3O_4 MNPs	10	127	7.0	67.56	75.56	24.44	8.5

preparation and characterization of Fe_3O_4 MNPs were supplied in Supplementary material. The physiochemical properties of Fe_3O_4 MNPs are listed in Table 1.

2.1. Batch experiments

The batch experiments were carried out in 100 mL polypropylene bottles containing 50 mL of aqueous solution. The concentration of adsorbent was $0.05\,g\,L^{-1}$ and the corresponding solid-to-liquid ratio was $1{:}2 \times 10^4$. Ionic strength was adjusted with 1 M NaCl solution, and solution pH was adjusted with HCl and NaOH. The suspension was stirred at 200 rpm at room temperature for 24 h. The residual concentration of CTC in supernatant was analyzed with HPLC-UV system (The detailed analytical method for CTC was presented in Supplementary material.). Adsorption kinetic study was performed following the above adsorption procedure at certain intervals of time at pH 6.5. The effect of solution pH was investigated at pH 3–11. The influence of ionic strength (10, 20 and 50 mM) and coexisting cations (Mg^{2+}, Ca^{2+}) were tested at pH 6.5 by adding NaCl, $MgCl_2$ and $CaCl_2$, respectively. The effect of HA was investigated by changing the concentration of HA from 2 to $50\,mg\,L^{-1}$ with the initial concentration of CTC fixed at $8\,mg\,L^{-1}$ at pH 6.5. The adsorption of CTC on Fe_3O_4 MNPs in several environmental water samples was tested by fixing the initial concentration of CTC at $5\,mg\,L^{-1}$. All experiments were conducted in triplicate, and average results were reported.

2.2. Regeneration of adsorbents

The regeneration of Fe_3O_4 MNPs was carried out by desorbing CTC from adsorbent with acid, alkaline or EDTA–Mcilvaine solution. In addition, we tried to directly destroy the adsorbed CTC on Fe_3O_4 MNPs surface by calcining the particles at 400 °C for 3 h under the protection of N_2 [19], or soaking the particles in 2 mL H_2O_2 (25%) for 6 h.

2.3. Adsorption model

The linear equation and Langmuir equation were used to describe the adsorption process of CTC on Fe_3O_4.

$$q_e = K_d C_e \tag{1}$$

$$q_e = \frac{Q_m K_L C_e}{1 + K_L C_e} \tag{2}$$

where Q_m ($mg\,g^{-1}$) is the maximum adsorption capacity, q_e ($mg\,g^{-1}$) is the amount of equilibrium adsorbed CTC, C_e ($mg\,L^{-1}$) is the equilibrium solute (CTC) concentration, K_L ($L\,mg^{-1}$) is the binding constant of CTC on adsorbent, and K_d ($L\,g^{-1}$) is the linear adsorption coefficient. The Langmuir model assumes that the adsorption occurs through monolayer adsorption on homogeneous surface without transformation and interaction between the adsorbed adsorbate. The K_d of linear isotherm model suggests apparent partition of organic pollutants in two phases.

3. Results and discussion

3.1. CTC adsorption kinetics

The adsorption of CTC on Fe_3O_4 MNPs was very fast, and about 95% of CTC adsorption happened in the first 60 min. The adsorption equilibrium was achieved at 600 min (Fig. 1), which was slower than the adsorption rate of TCs on palygorskite (2 h) [20], but much faster than that on rectorite (20 h) [12], aluminum and iron hydrous oxides (180 h) [14], micro- and mesoporous carbons (3 d) [21]. The kinetics of CTC adsorption on Fe_3O_4 was analyzed using the pseudo-second-order model, a commonly used model that describes chemisorption process of organic pollutants from aqueous solution [22].

$$q_t = \frac{kq_e^2 t}{1 + kq_e t} \tag{3}$$

where k ($g\,mg^{-1}\,h^{-1}$) is the rate constant of the pseudo-second-order adsorption, kq_e^2 ($t \to 0$) is initial adsorption rate ($mg\,g^{-1}\,h^{-1}$), q_e ($mg\,g^{-1}$) and q_t ($mg\,g^{-1}$) are the amount of CTC adsorbed at equilibrium and t time, respectively. Eq. (3) can be rearranged to:

$$\frac{t}{q_t} = \frac{t}{q_e} + \frac{1}{kq_e^2} \tag{4}$$

Based on linear regression ($R^2 > 0.9999$) value of plotting of t/q_t against t, the kinetics of CTC adsorption onto Fe_3O_4 fitted well with the pseudo-second-order kinetics model (Fig. 1, inset). The constant k and initial adsorption rate kq_e^2 obtained from the slope and intercept of plot were $0.064\,g\,mg^{-1}\,h^{-1}$ and $714\,mg\,g^{-1}\,h^{-1}$, respectively. The calculated q_e was $105.26\,mg\,g^{-1}$, which agreed well with the experimental data at $t = 600$ min.

3.2. Effect of solution pH

It was reported that solution pH played an important role on CTC adsorption to metal oxides [10,15]. Similarly, the adsorption of CTC on Fe_3O_4 MNPs was also pH-dependent. As shown in Table 2, the adsorption capacity of CTC increased with solution pH at pH

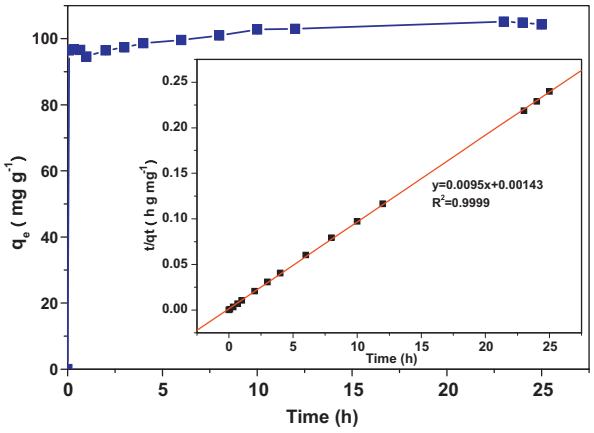

Fig. 1. Adsorption kinetic of CTC on Fe_3O_4 MNPs. Inset describes the liner plot of Eq. (4). $C_{sorbent} = 0.05\,g\,L^{-1}$; pH = 6.5; $T = 298$ K; $C_{NaCl} = 10$ mM; $C_{CTC} = 5\,mg\,L^{-1}$.

Table 2
Langmuir isotherms and linear adsorption isotherms parameters for CTC adsorption at different solution pH. $C_{sorbent}$ = 0.05 g L^{-1}; T = 298 K; C_{NaCl} = 10 mM.

pH	Langmuir model			Linear model		Monolayer adsorption density (CTC $(nm^2)^{-1}$)
	Q_m (mg g^{-1})	K_L (L mg^{-1})	R^2	K_d (L g^{-1})	R^2	
3.0	186	12,251	0.944	7.57	0.967	1.43
4.5	276	12,567	0.998	10.5	0.993	2.90
5.5	377	12,368	0.985	11.9	0.993	3.65
6.5	476	23,051	0.951	14.5	0.990	4.69
7.5	258	9715	0.994	9.04	0.995	2.53
8.5	187	14,573	0.987	5.56	0.932	1.70

3.5–6.5, but decreased with further increase of pH (pH 6.5–8.5). The observed pH dependence could be rationalized by evaluating the charges of CTC and Fe_3O_4 surfaces. The zero-point-of-charge (pH_{pzc}) of Fe_3O_4 MNPs was pH 7.0 (Table 1). Therefore, Fe_3O_4 was positively charged at pH < 7.0 and negatively charged at pH > 7.0. The pK_a of CTC molecule was 3.3, 7.44, 9.27, respectively [23] (Fig. S1). CTC existed as cationic ions in strong acid solution, zwitter anions at 3.3 < pH < 7.44, and negative ions at pH > 7.44 [23,24]. Electrostatic repulsion between CTC and Fe_3O_4 surface was lowest at pH near to pH = (pK_{a1} + pK_{a2})/2. Therefore, the greatest adsorption of CTC on Fe_3O_4 MNPs was observed at pH 5–7.

At pH 6.5, the maximal adsorption capacity of CTC on Fe_3O_4 was 476 mg g^{-1}. This value was much higher than the adsorption capacities of TCs on minerals or metal oxides such as rectorite (140 mg g^{-1}) [12], palygorskite (61.8 mg g^{-1}) [20], and marine sediments (16.7–33.3 mg g^{-1}) [13]. The K_d value of linear adsorption isotherms was 14.5 L g^{-1}, which was higher than that achieved on activated sludge (8.4 L g^{-1}) [25], and soil organic matter (1.14–1.62 L g^{-1}) [26].

3.3. Effect of temperature

Since degradation or transformation of CTC in solution was observed as the temperature was higher than 313 K in the control experiment, the effect of temperature on CTC adsorption was investigated at 298, 303 and 313 K. The adsorption enhanced with increase of temperature, and the maximal adsorption capacity of CTC on Fe_3O_4 increased by 10% and 40% at 303 K and 313 K, respectively, compared with that at 298 K (Fig. 2a).

The Gibbs energy of the adsorption process could be calculated from the CTC adsorption coefficient (K_d) between solid and solution.

$$\Delta G = -RT \ln K_d \quad (5)$$

The changes of enthalpy and entropy of CTC adsorption were obtained from the equation as follows:

$$\ln K_d = -\frac{\Delta H}{RT} + \frac{\Delta S}{R} \quad (6)$$

where ΔH is the change in enthalpy, ΔS is the change in entropy, T is the reaction temperature in K, and R = 8.314 J (mol K)$^{-1}$. The $\ln K_d$ and $1/T$ fitted the Van't Hoff linear (R^2 = 0.959) equation; ΔH and ΔS were obtained from the slope and intercept of a plot of $\ln K_d$ versus $1/T$ (Fig. S2). The thermodynamic parameters of CTC adsorption were presented in Table S1.

The negative value of Gibbs energy (ΔG) indicated that the adsorption was spontaneous. The absolute value of ΔG increased with the increase of temperature, which implied that higher temperature facilitated the adsorption of CTC on Fe_3O_4 MNPs. The positive ΔS (0.21 J (mol K)$^{-1}$) informed that the adsorption was an irreversible process. The value of ΔH was positive suggesting that the reaction was endothermic. If the ΔH is higher than 40 kJ mol^{-1}, the adsorption process is supposed to proceed via chemisorption; while for values less than 40 kJ mol^{-1}, the adsorption process is of physical nature [27]. The value of ΔH was 57.7 kJ mol^{-1}. Therefore, we proposed that the main interaction between CTC and Fe_3O_4 MNPs was chemisorption.

3.4. Effect of ionic strength and coexisting ions

Effect of ionic strength on CTC adsorption was investigated by performing adsorption equilibrium experiments at different concentrations of NaCl at pH 6.5. As a result, the adsorption capacity was decreased by 2–4% when the concentration of NaCl increased from 10 mM to 50 mM (Fig. 2b). This suggested that surface complexation of CTC with Fe_3O_4 was stronger than non-specific electrostatic interactions [15].

Since CTC strongly forms complex with multivalent cations, the influence of coexisting foreign cations was tested. The adsorption of CTC changed insignificantly when the concentration of Ca^{2+} and Mg^{2+} was in the range of 2–4 mM (50–100 mg L^{-1}) (Fig. 2c). However, the adsorption of CTC was totally inhibited when the concentration of the two cations was increased to 10 mM. In real water samples, the concentration of Ca^{2+} and Mg^{2+} cations was generally less than 100 mg L^{-1}. Therefore, we expected that the adsorption of CTC on Fe_3O_4 MNPs would not be affected by these coexisting cations in practical application.

3.5. Effect of HA

The effect of HA on CTC adsorption was also investigated. The results were shown in Fig. 2d. Without HA in aqueous solution, the amount of CTC adsorbed on Fe_3O_4 was 102.6 mg g^{-1}. In the presence of 2 mg L^{-1} of HA, the adsorbed CTC decreased to 76.1 mg g^{-1}. With the increase of HA concentration, the adsorption of CTC increased gradually. As the concentration of HA increased to 30 and 50 mg L^{-1}, the amount of adsorbed CTC was 118 and 126 mg g^{-1}, respectively.

Illés reported that HA was hardly adsorbed by Fe_3O_4 MNPs and remained free in solution as the concentration of HA was lower than 2.8 mg L^{-1} [28]. The free HA also had a strong affinity to TCs [29]. Therefore, in this study the presence of 2 mg L^{-1} of HA in reaction solution significantly decreases the adsorption of CTC on Fe_3O_4 MNPs due to the competitive adsorption between Fe_3O_4 MNPs adsorbent and HA to CTC. With the increase of HA concentration in solution, however, HA tends to adsorb on the surface of Fe_3O_4 MNPs. Both Fe_3O_4 MNPs and the sorbed HA on Fe_3O_4 MNPs surface can serve as potent adsorbent to adsorb CTC, which is the possible reason for the gradually increased CTC adsorption as the coexisting HA enhanced from 2 to 50 mg L^{-1}.

3.6. Effect of environmental matrix

Two influent and effluent water samples of two sewage treatment plants, a tap water sample and a seawater sample were used to study the effect of sample matrix on CTC adsorption. The

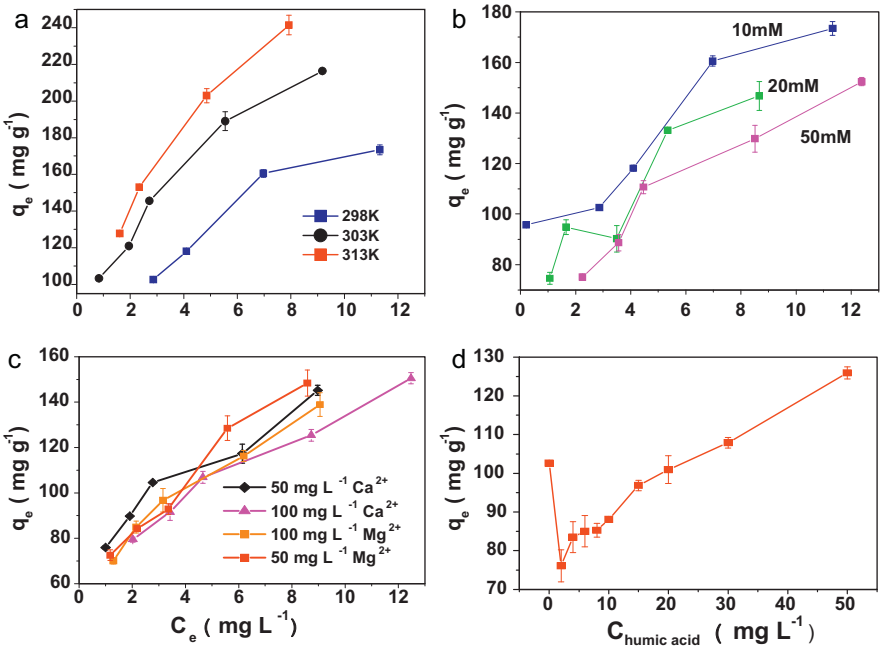

Fig. 2. Effect of temperature (a), ionic strength (b), coexisting Ca^{2+}, Mg^{2+} cations (c), and humic acid (d) on CTC adsorption onto Fe_3O_4 MNPs. $C_{sorbent}$ = 0.05 g L^{-1}; pH = 6.5.

amount of CTC adsorbed on Fe_3O_4 MNPs in effluent water samples and tap water sample was similar with that obtained in deionized water. The adsorbed amount of CTC on Fe_3O_4 in influent samples decreased only 7% compared with that in deionized water. However, the CTC adsorption decreased to 75.6% in seawater sample due to the high salinity (Fig. 3). Generally, the effect of environmental matrixes on CTC adsorption was not evident, which indicated that Fe_3O_4 MNPs were excellent adsorbents to remove CTC from environment water samples (especially for surface water).

3.7. Regeneration of Fe_3O_4 MNPs

The regeneration tests showed that neither acid (pH 3.5) nor alkaline (pH 10) solution could elute the adsorbed CTC efficiently from Fe_3O_4 MNPs. In EDTA–Mcilvaine solution, though CTC could be recovered, the Fe_3O_4 nanoparticles were dissolved into the solution completely. After calcination or H_2O_2 oxidation treatment of Fe_3O_4 MNPs with adsorbed CTC, the solid was also dissolved by EDTA–Mcilvaine solution to detect the residual CTC. As a result, no CTC was detected after heat treatment, and the C element could not be found on the surface of calcined Fe_3O_4 (Table S2), indicating the complete removal of CTC from Fe_3O_4 surface. After treatment with H_2O_2, less than 2% of residual CTC was detected in EDTA–Mcilvaine solution, and the C element content was about 8% on the surface of H_2O_2–Fe_3O_4. The efficiency of CTC removal by the regenerated adsorbents was also studied (Fig. S3). The maximum adsorption capacity of CTC was 476 mg g^{-1}, 769 mg g^{-1} and 588 mg g^{-1} on Fe_3O_4 MNPs, calcined Fe_3O_4 MNPs and H_2O_2–Fe_3O_4 MNPs, respectively. The increased adsorption of CTC onto the regenerated Fe_3O_4 might be caused by the possible transformation between the Fe(II) and Fe(III) species on Fe_3O_4 surface during the calcination in N_2 atmosphere or H_2O_2 oxidation treatment, and Fe(III) should possess stronger tendency to form complex with CTC than Fe(II). However, the crystal structure (Fig. S4), particle size (Fig. S5) and physical properties were kept unchanged (Table S2), suggesting that the change of Fe_3O_4 MNPs surface was negligible during the regeneration process. These results indicated that Fe_3O_4 MNPs could be successfully regenerated through these two methods.

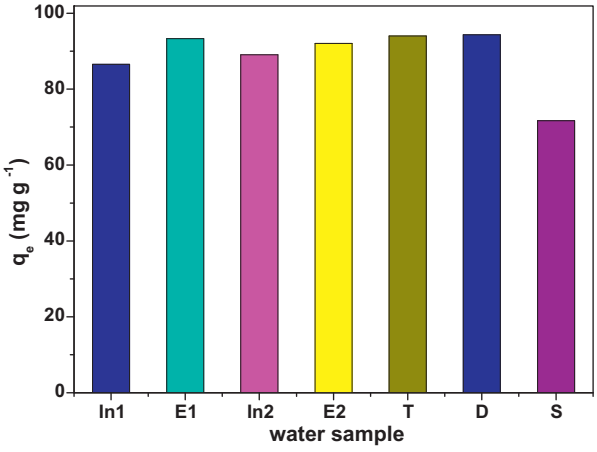

Fig. 3. The adsorption of CTC on Fe_3O_4 MNPs in different water samples. I1, E1, I2 and E2 represents the influent and effluent water in different sewage treatment plants; T, D, and S represents tap water, deionized water, and seawater, respectively. $C_{sorbent}$ = 0.05 g L^{-1}; pH = 6.5; T = 298 K; C_{CTC} = 5 mg L^{-1}.

3.8. Surface complexation

To confirm the complexation of CTC with Fe_3O_4 surface, 10 mM EDTA, an excellent chelating agent with multivalent ions, was added into the reaction solution. Consequently, the adsorption capacity of CTC on Fe_3O_4 was decreased by 50% due to the chelation between EDTA and Fe species on Fe_3O_4 surface. XPS measurements were carried out to study the chemical state of Fe on Fe_3O_4 surface before and after CTC adsorption. The XPS spectra of Fe $2p_{3/2}$ was composed of overlapped peaks of Fe(II) and Fe(III). Compared with bare Fe_3O_4, the peak of the Fe $2p_{3/2}$ spectra had shifted to more negative binding energy after adsorption of CTC, and the shift degree for Fe(II) and Fe(III) was −0.13 eV and −0.11 eV, respectively (Fig. 4). The decrease of the binding energy of iron indicated the increase of their electron density, resulting from the formation of Fe–O bonds through complexation between CTC and Fe atoms.

Schmitt and Schneider [11] reported that the binding constants of metal/CTC complexes determined from spectroscopic investi-

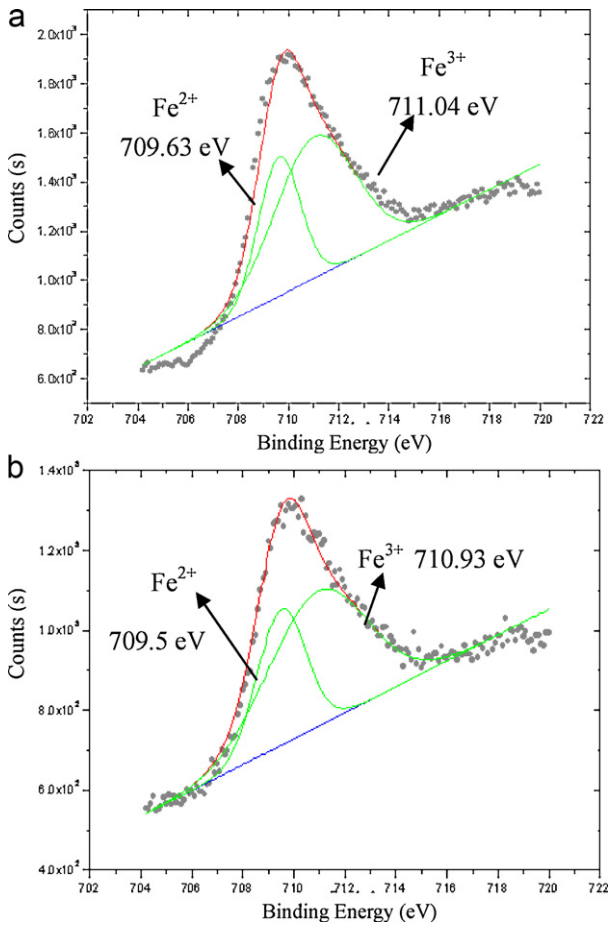

Fig. 4. The XPS of Fe 2p3/2 peaks of Fe_3O_4 nanoparticles before (a) and after (b) CTC adsorption.

gations refer to the consecutive formation of a 1:1 and a 2:1 M^{2+}–TC complex in aqueous solution. According to the two-step adsorption kinetics shape and low Langmuir monolayer adsorption density of CTC on iron oxide-coated quartz, Tanis et al. [15] suggested that the 1:1 type Fe–CTC complexes was transmitted to 2:1 type at equilibrium. In this study, the adsorbed density of CTC on Fe_3O_4 MNPs was calculated using the surface area of Fe_3O_4 and the molecular weight of CTC. In neutral solution (pH 6.5) at 25 °C, the Langmuir monolayer adsorption capacity was 4.7 CTC per nm^2 (7.8 μmol $(m^2)^{-1}$) (Table 2), which was ten times larger than that obtained on iron oxide-coated quartz (0.7 μmol $(m^2)^{-1}$). The surface density of hydroxyl groups on Fe_3O_4 (particle size 9 nm, surface area 123 $m^2\,g^{-1}$) was found to be 8.5 OH per nm^2 [30]. Since the density of OH groups was in the order of the density of Fe atoms exposed on the regular Fe_3O_4(1 1 1) surface [31], we hypothesized that density of Fe(II) + Fe(III) was approximately equal to 8.5 Fe/nm^2 (Table 1). Considering the fast adsorption dynamic of CTC and the steric effect among CTC on Fe_3O_4 surface, we proposed that the 1:1 type Fe–CTC complexes were dominantly formed.

The adsorption of tetracycline (TC), oxytetracycline (OTC), quinolones (ofloxacin) and sulfonamides (sulfathiazole) on Fe_3O_4 MNPs were also investigated. As a result, both TC and OTC had strong adsorption ability to Fe_3O_4 MNPs. Under the optimal conditions, the maximum adsorption capacities of TC and OTC on Fe_3O_4 MNPs were 500 mg g^{-1} and 526 mg g^{-1}, respectively and the adsorption equilibrium was achieved at 720 min (Fig. S6). However, ofloxacin and sulfathiazole showed weak affinity to Fe_3O_4 MNPs and the adsorption capacity was less than 10 mg g^{-1} in the whole pH range (Fig. S7). These results suggest the possibility of selective removal of TCs from aqueous media by using Fe_3O_4 MNPs.

4. Conclusions

The adsorption of chlorotetracycline on Fe_3O_4 MNPs was studied. CTC adsorption reached equilibrium within 10 h and the adsorption kinetics fitted well to the pseudo-second-order model equation. The optimal adsorption of CTC was observed at pH 6.5, and the maximal Langmuir adsorption capacity was 476 mg g^{-1} (7.8 μmol $(m^2)^{-1}$). The adsorption of CTC was insignificantly affected by ions strength and low concentration of coexisting Ca^{2+} and Mg^{2+}. The effect of HA on CTC adsorption was found to be concentration-dependent. Fe_3O_4 MNPs remained excellent adsorption ability to CTC in several environmental water samples and were regenerated by calcination at 400 °C under N_2 protection or treatment with H_2O_2. The regenerated Fe_3O_4 MNPs possessed higher adsorption affinity to CTC than the original Fe_3O_4. Surface complexation of CTC with Fe_3O_4 was confirmed by the competing adsorption of EDTA and XPS spectra of adsorbent. Anyway, the results presented here suggested the potential of Fe_3O_4 MNPs as an efficient material to remove TCs selectively from water samples.

Acknowledgments

This work was jointly supported by National Basic Research Program of China (2010CB933500) and the National Natural Science Foundation of China (20837003, 20890111, 20921063).

Appendix A. Supplementary data

Supplementary data associated with this article can be found, in the online version, at doi:10.1016/j.jhazmat.2011.06.015.

References

[1] K. Kümmerer, Antibiotics in the aquatic environment—a review. Part I, Chemosphere 75 (2009) 417–434.
[2] N. Wu, M. Qiao, B. Zhang, W.D. Cheng, Y.G. Zhu, Abundance and diversity of tetracycline resistance genes in soils adjacent to representative swine feedlots in China, Environ. Sci. Technol. 44 (2010) 6933–6939.
[3] M.E. Lindsey, M. Meyer, E.M. Thurman, Analysis of trace levels of sulfonamide and tetracycline antimicrobials, in ground water and surface water using solid-phase extraction and liquid chromatography/mass spectrometry, Anal. Chem. 73 (2001) 4640–4646.
[4] K.D. Brown, J. Kulis, B. Thomson, T.H. Chapman, D.B. Mawhinney, Occurrence of antibiotics in hospital, residential, and dairy effluent, municipal wastewater, and the Rio Grande in New Mexico, Sci. Total Environ. 366 (2006) 772–783.
[5] K.G. Karthikeyan, M. Meyer, Occurrence of antibiotics in wastewater treatment facilities in Wisconsin, USA, Sci. Total Environ. 361 (2006) 196–207.
[6] L.H. Santosa, A.N. Araújoa, A. Fachinia, A. Penab, C. Delerue-Matosc, M.C.B.S.M. Montenegro, Ecotoxicological aspects related to the presence of pharmaceuticals in the aquatic environment, J. Hazard. Mater. 175 (2010) 45–95.
[7] A. Jindal, S. Kocherginskaya, A. Mehboob, M. Robert, R.I. Mackie, L. Raskin, J.L. Zilles, Antimicrobial use and resistance in swine waste treatment systems, Appl. Environ. Microbiol. 72 (2006) 7813–7820.
[8] S.P. Kim, H.K. Park, K. Chandran, Propensity of activated sludge to amplify or attenuate tetracycline resistance genes and tetracycline resistant bacteria: a mathematical modeling approach, Chemosphere 78 (2010) 1071–1077.
[9] D. Ferber, From pigs to people: the emergence of a new superbug, Science 329 (2010) 1010–1011.
[10] W.R. Chen, C.H. Huang, Adsorption and transformation of tetracycline antibiotics with aluminum oxide, Chemosphere 79 (2010) 779–785.
[11] D.L. Schmitt, S. Schneider, Spectroscopic investigation of complexation between various tetracyclines and Mg^{2+} or Ca^{2+}, PhysChemComm 3 (2000) 42–55.
[12] P.H. Chang, J.S. Jean, W.T. Jiang, Z.H. Li, Mechanism of tetracycline sorption on rectorite, Colloids Surf. A 339 (2009) 94–99.
[13] X.R. Xu, X.Y. Li, Sorption and desorption of antibiotic tetracycline on marine sediments, Chemosphere 78 (2010) 430–436.
[14] C. Gu, Interaction of tetracycline with aluminum and iron hydrous oxides, Environ. Sci. Technol. 39 (2005) 2660–2667.
[15] E. Tanis, K. Hanna, E. Emmanuel, Experimental and modeling studies of sorption of tetracycline onto iron oxides-coated quartz, Colloids Surf. A 327 (2008) 57–63.

[16] M. Iram, C. Guo, Y.P. Guan, A. Ishfaq, H.Z. Liu, Adsorption and magnetic removal of neutral red dye from aqueous solution using Fe_3O_4 hollow nanospheres, J. Hazard. Mater. 181 (2010) 1039–1050.
[17] Y.F. Shen, J. Tang, Z.H. Nie, Y.D. Wang, Y. Ren, L. Zuo, Preparation and application of magnetic Fe_3O_4 nanoparticles for wastewater purification, Sep. Purif. Technol. 68 (2009) 312–319.
[18] S.X. Zhang, H.Y. Niu, Y.Q. Cai, X.L. Zhao, Y.L. Shi, Arsenite and arsenate adsorption on coprecipitated bimetal oxide magnetic nanomaterials: $MnFe_2O_4$ and $CoFe_2O_4$, J. Chem. Eng. 158 (2010) 599–607.
[19] X.J. Peng, Z.K. Luan, H.M. Zhang, Montmorillonite–Cu(II)/Fe(III) oxides magnetic material as adsorbent for removal of humic acid and its thermal regeneration, Chemosphere 63 (2006) 300–306.
[20] P.H. Chang, Z.H. Li, T.L. Yu, S. Munkhbayer, T.H. Kuo, Y.C. Hung, J.S. Jean, K.H. Linc, Sorptive removal of tetracycline from water by palygorskite, J. Hazard. Mater. 165 (2009) 148–155.
[21] L.L. Ji, F.L. Liu, Z.Y. Xu, S.R. Zheng, D.Q. Zhu, Adsorption of pharmaceutical antibiotics on template-synthesized ordered micro- and mesoporous carbons, Environ. Sci. Technol. 44 (2010) 3116–3122.
[22] Z. Eren, F.N. Acar, Adsorption of reactive black 5 from an aqueous solution: equilibrium and kinetic studies, Desalination 194 (2006) 1–10.
[23] C.K. Stephen, S.K. Muraik, J. Bruningas, K.B. Woodwarl, Acidity constants of tetracyline antibiotics, J. Am. Chem. Soc. 78 (1956) 4155–4158.
[24] Z. Qiang, C. Adams, Potentiometric determination of acid dissociation constants (pK_a) for human and veterinary antibiotics, Water Res. 38 (2004) 2874–2890.
[25] S. Kim, P. Eichhorn, J.N. Jensen, A.S. Weber, D.S. Aga, Removal of antibiotics in wastewater: effect of hydraulic and solid retention times on the fate of tetracycline in the activated sludge process, Environ. Sci. Technol. 39 (2005) 5816–5823.
[26] S.A. Sassman, L.S. Lee, Sorption of three tetracyclines by several soils: assessing the role of pH and cation exchange, Environ. Sci. Technol. 39 (2005) 7452–7459.
[27] B.G. Whitehouse, The effects of temperature and salinity on the aqueous solubility of polynuclear aromatic hydrocarbons, Mar. Chem. 4 (1984) 319–332.
[28] E. Illés, E. Tombácz, The effect of humic acid adsorption on pH-dependent surface charging and aggregation of magnetite nanoparticles, J. Colloid Interface Sci. 295 (2006) 115–123.
[29] C. Gu, K.G. Karthikeyan, S.D. Sibley, J.A. Pedersen, Complexation of the antibiotic tetracycline with humic acid, Chemosphere 66 (2007) 1494–1501.
[30] I. Garcia, N.E. Zafeiropoulos, A. Janke, A. Tercjak, A. Eceiza, M. Stamm, I. Mondragon, Functionalization of iron oxide magnetic nanoparticles with poly (methyl methacrylate) brushes via grafting-from atom transfer radical polymerization, J. Polym. Sci. Polym. Chem. 45 (2007) 925–932.
[31] Y. Joseph, W. Ranke, W. Weiss, Water on FeO(1 1 1) and Fe_3O_4(1 1 1): adsorption behavior on different surface terminations, J. Phys. Chem. B 104 (2000) 3224–3236.